Shear strength of sand under different range of confining stresses using various shearing devices

Vivoda Prodan, M.; Peranić, J.; Jagodnik, V.; Marušić, D.; Štiberc, D.; Kamenar, N.; Arbanas, Ž.

Proceedings of the XVIII ECSMGE 2024
GEOTECHNICAL ENGINEERING CHALLENGES
TO MEET CURRENT AND EMERGING NEEDS OF SOCIETY

ISBN 978-1-032-54816-6
DOI 10.1201/9781003431749-252

ECSMGE 24
XVIII EUROPEAN CONFERENCE ON SOIL MECHANICS AND GEOTECHNICAL ENGINEERING

Shear strength of sand under different range of confining stresses using various shearing devices

Résistance au cisaillement du sable sous différentes plages de contraintes de confinement à l'aide de divers dispositifs de cisaillement

M. Vivoda Prodan*, J. Peranić, V. Jagodnik, D. Marušić, D. Štiberc, N. Kamenar, Ž. Arbanas
Faculty of Civil Engineering University of Rijeka, Rijeka, Croatia

**martina.vivoda@gradri.uniri.hr*

ABSTRACT: Small-scale slope modelling is being conducted at the Faculty of Civil Engineering, University of Rijeka, to investigate various aspects of landslides triggered by rainfall, such as effects of initial soil moisture and soil hydraulic properties, the characteristics and patterns of rainfall on the hydro-mechanical response of slopes, and the physical processes and mechanisms driving the initiation and propagation of rainfall-induced landslides, as well as the effectiveness of various remediation measures. Understanding the test results of the physical slope model requires, among others, knowledge of the shear strength properties of the soil(s) forming the model. This study comprises a series of laboratory tests to investigate the shear strength of clean sand used as a base soil material for the construction of slope models. A series of laboratory shear tests were performed using conventional direct shear, triaxial and ring shear devices under a wide range of confining stresses, including low confining stresses typically present in 1g model tests. The strain-controlled tests were performed on sand samples installed at the same density conditions representative to the sand material used in the small-scale slope physical models and under stress conditions representative in small-scale and real slopes.

RÉSUMÉ: Une modélisation des pentes à petite échelle est actuellement menée à la Faculté de génie civil de l'Université de Rijeka pour étudier divers aspects des glissements de terrain déclenchés par les précipitations, tels que l'effet de l'humidité initiale du sol et de ses propriétés hydrauliques, les caractéristiques et les régimes des précipitations sur le sol, la réponse hydromécanique des pentes et, les processus, les mécanismes physiques à l'origine de l'initiation et de la propagation des glissements de terrain induits par les précipitations, ainsi que l'efficacité des diverses mesures d'assainissement. Comprendre les résultats des tests du modèle physique de pente nécessite, entre autres, la connaissance des propriétés de résistance au cisaillement du ou des sols formant le modèle. Cette étude comprend une série d'essais en laboratoire visant à étudier la résistance au cisaillement du sable propre utilisé comme matériau de base pour la construction de modèles de pente. Une série d'essais de cisaillement en laboratoire ont été réalisés à l'aide de dispositifs conventionnels de cisaillement direct, triaxial et annulaire sous une large gamme de contraintes de confinement, y compris les faibles contraintes de confinement généralement présentes dans les essais sur modèle 1g. Les tests de déformation contrôlée ont été effectués sur des échantillons de sable installés dans les mêmes conditions de densité représentatives du matériau sableux utilisé dans les modèles physiques de pente à petite échelle et dans des conditions de contrainte représentatives des pentes à petite échelle et réelles.

Keywords: Landslides; laboratory testing; shear strength; low effective confining stresses.

1 INTRODUCTION

Landslides are among the greatest geohazards and are being studied in a variety of fields worldwide, including landslide modelling and landslide remediation.

A research project funded by the Croatian Science Foundation entitled "Physical modelling of landslide remediation constructions behaviour under static and seismic actions" was a part of extensive research on small-scale slopes. The main task of the project was to compare the responses of scaled slope models from different soil types and geometric conditions with and without remediation measures subjected to different loading conditions - static (rainfall-triggered landslide) and seismic (earthquake-triggered landslide) instrumented with geodetic and geotechnical monitoring equipment. More on the tests performed on the physical model can be found in Jagodnik & Arbanas (2022); Pajalić et al. (2021); Peranić et al. (2022); Vivoda Prodan et al. (2023).

The shear strength of sand at low confining stresses present in small-scale slope physical model needs to be investigated. One of the pioneering researches on the shear strength of sands at low confining stresses

was done by Ponce & Bell (1971). The authors have registered the dilatative behaviour of loose sands at low confining stresses, similar to dense sands' behaviour at moderate confining stresses. General shear strength and dilatative characteristics of saturated sands at low confining stress were further investigated and presented by Fukushima & Tatsuoka (1984). Shaoli et al. (2003) studied the undrained behaviour of sand under low confining stresses, and found that static liquefaction in such conditions is dominantly governed by the sand's relative density. Laurent et al. (2006) showed in their research that at low confining stresses, the sands' friction and dilatancy angle are stress-dependent. Finally, Chakraborty & Salgado (2010) used a series of triaxial compression and plane-strain compression data results to analyze the dependence of dilatancy and friction angle on sand specimens' relative density and confining stress. Winters et al. (2016) found that a better representation of the relationship between shear stress and normal stress can be found by curving the failure envelope at low confining pressures.

Based on an extensive literature showing the differences between the results that can be obtained with different devices (Castellanos & Brandon, 2013; Cuomo et al., 2016; Vivoda Prodan et al., 2016), different test devices were used in this study.

The ring shear tests were conducted using the ICL-1 ring shear device, (Marui & Co., Ltd., Osaka, Japan) developed in 2010 (Figure 1a), which can simulate the formation of the landslide sliding surface with the following post-failure motion, observe the consequence of mobilized shear resistance and the post-failure shear displacement as well as the generated pore water pressure. The ICL-1 can perform stress (monotonic, dynamic, seismic), strain and pore water pressure controlled tests in drained or undrained conditions. It can maintain a pore water pressure of up to 1 MPa and apply a normal stress of up to 1 MPa, making it suitable for investigation of large-scale and deep-seated landslides. The cylindrical sample has an inner and outer diameter of 10 and 14 cm, respectively and a maximum height of 5.2 cm. The maximum and minimum shear rate is 5.4 and 0.01 cm/s, respectively and cyclic torque control tests can be performed at a maximum frequency of 1.0 Hz (Oštrić et al., 2014). Vivoda Prodan et al. (2016); Vivoda Prodan & Arbanas (2020) investigated the influence of the weathering process on the shear strength of siltstones from a flysch rock mass on the northern Adriatic coast of Croatia using the ICL-1.

Direct shear tests were performed using the Back Pressured Shear Box (GDS Instruments Ltd., London, United Kingdom), (Figure 1b). The device enables the testing of square soil samples in a saturated or partially saturated state with the dimensions 100x100x30 mm at a maximum normal force of 10 kN and a maximum shear force of 5 kN. The maximum shear displacement is ±12.5 mm, while the maximum working back pressure that can be applied is 1 MPa. The device was used by Peranić et al. (2020) to perform standard, strain-controlled tests on undisturbed samples of residual soil from flysch rock mass in unsaturated (i.e. suction-controlled) and saturated conditions. Peranić & Arbanas (2020) used the same device to investigate the behaviour of the soil when undergoing the wetting process.

Static triaxial tests were performed using the Wykeham Farrance static triaxial system (Figure 1c). Tests were performed on a sample with a height to diameter ratio of 100/50 mm. The maximum pressure capacity of the static triaxial system is 1 MPa, the load cell used had a maximum force of 25 kN. The maximum axial displacement is 50 mm (Jagodnik et al., 2020).

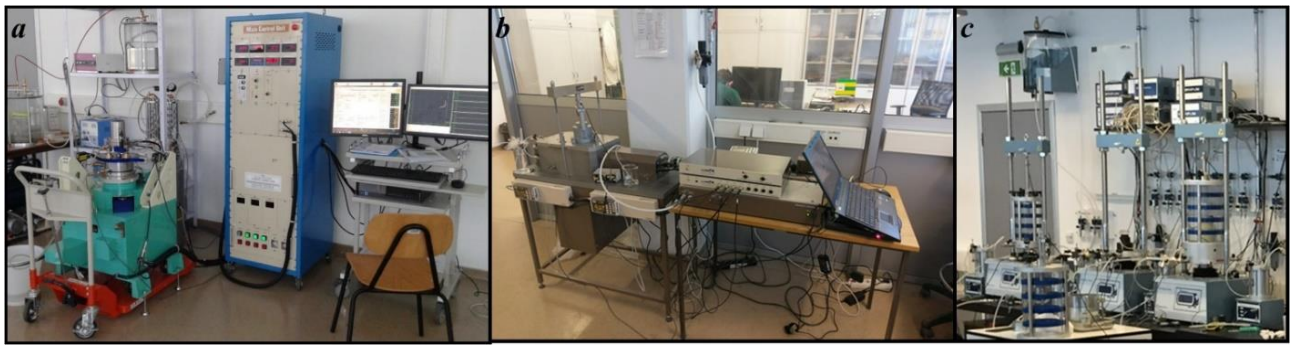

Figure 1. Devices at the Geotechnical laboratory at the Faculty of Civil Engineering University of Rijeka to determine shear strength of sand: a) ring shear (RS) device, b) back pressurized direct shear (DS) device for soil testing in saturated and unsaturated conditions, c) triaxial (TX) device.

The focus of this study is to investigate the shear strength properties of a uniformly graded fine sand used in physical slope modelling. So far, a series of laboratory tests were carried out using direct shear,

triaxial and ring shear devices under a wide range of confining stresses, including relatively low values of stresses representative for the 1g modelling tests.

2 LABORATORY TESTING

Barotropy, i.e. the dependence of the mechanical behaviour of the soil on the stress level, is known to be one of the greatest limitations in a use of small-scale physical models under 1g conditions. The main objective of conducted laboratory tests is to establish relationships between soil material behaviour in a small-scale model and a prototype, i.e., a real slope in a field.

2.1 Sand properties

The fine-grained (0–1 mm) Drava River sand was selected as the base material to represent cohesionless slopes. Figure 2 shows the physical model after the installation of the material and monitoring equipment. The basic physical properties of the described material are given in Table 1.

Figure 2. View of the small-scale physical model.

Table 1. Basic physical properties of the sand material built in the small-scale model.

Parameters	Values
Specific gravity, G_s	2.70
Dry density, ρ_d (g/cm^3)	1.52
Effective particle size	
D_{10} (mm)	0.19
D_{60} (mm)	0.37
Uniformity coefficient, c_u	1.947
Coefficient of curvature, c_c	1.092
Minimum void ratio, e_{min}	0.641
Maximum void ratio, e_{max}	0.911

2.2 Testing devices and methodology

Laboratory tests included direct shear (DS) tests, ring shear (RS) tests, and triaxial (TX) tests on the sandy material performed at the Geotechnical laboratory in the Faculty of Civil Engineering University of Rijeka, Croatia (Figure 1).

The samples were prepared under the same initial conditions as in the physical model, i.e. initial relative density of 50%, initial porosity equal to 0.44, and initial water content equal to 2%. Based on the known conditions related to the desired porosity, and an initial moisture of the tested samples, the mass of mixed sand and water installed in the devices was determined. After installation, samples were consolidated under a range of effective vertical stresses from 4 up to 200 kPa. The strain-controlled tests were performed under drained conditions with different strain rates, as presented in Table 2.

The ring shear box was filled with wet sand samples and then circulated with CO_2 and deaired distilled water. After consolidation at the effective vertical stresses in the range of 30 to 200 kPa with a back pressure of 15 to 50 kPa, shearing was performed at a shear rate of 0.01 cm/s.

Sand material was compacted in the shear box to achieve the sample height of 3 cm and the targeted porosity. Once the sample was installed, the chamber was filled with the deaired water and the sample was left to saturate in the following 24 hours period. After the saturation, the samples were consolidated under a range of confining stresses between 4 and 120 kPa. Finally, the samples were sheared at a low shear rate of 0.0087 mm/min to ensure drained response of the soil.

The samples for testing in the triaxial device were prepared using the undercompaction method, developed by Ladd (1978). The degree of undercompaction was 5%. To achieve faster saturation, the sample was percolated with CO_2 before water percolation. This assures that the Skemptons' *B* coefficient reaches value of 0.97, in average, after back pressurising. The rate of axial strain was 0.6 mm/min.

Table 2. List of the performed strain-controlled laboratory tests.

Device	Effective vertical stress (kPa)	Shear rate (cm/s)
RS	30, 60, 120, 200	0.01
DS	4, 8, 16, 30, 60, 120	1,44676E-05
TX	*16, 30, 60	**≈0.001

*** isotropic confining stress; ** rate of axial strain**

2.3 Test results

This section presents the results of performed drained tests with ring shear (RS), direct shear (DS) and triaxial (TX) devices on the uniform sand material. Figure 6 presents the peak and shear strength envelopes for steady-state conditions obtained in all

devices. The results are fitted using the Mohr-Coulomb strength criteria in σ'-τ plane.

Samples tested in the ring shear device show a tendency for compaction and then dilatation. The material experiences a sudden pronounced peak shear resistance followed by strain softening to the steady state (Figure 3). The residual shear strength envelope (Figure 6a) was obtained for the shear stress values corresponding to the maximum shear displacement reached during the tests, which could be infinite.

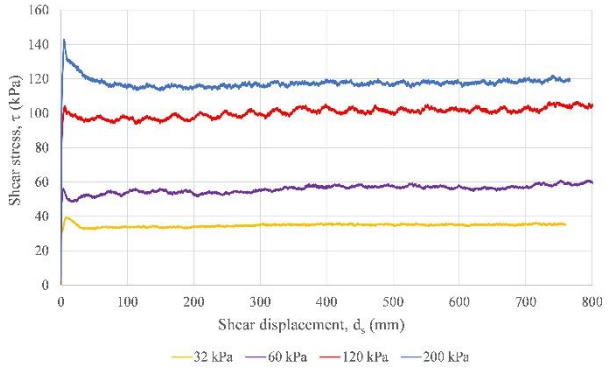

Figure 3. Shear stress-shear displacement of the RS tests.

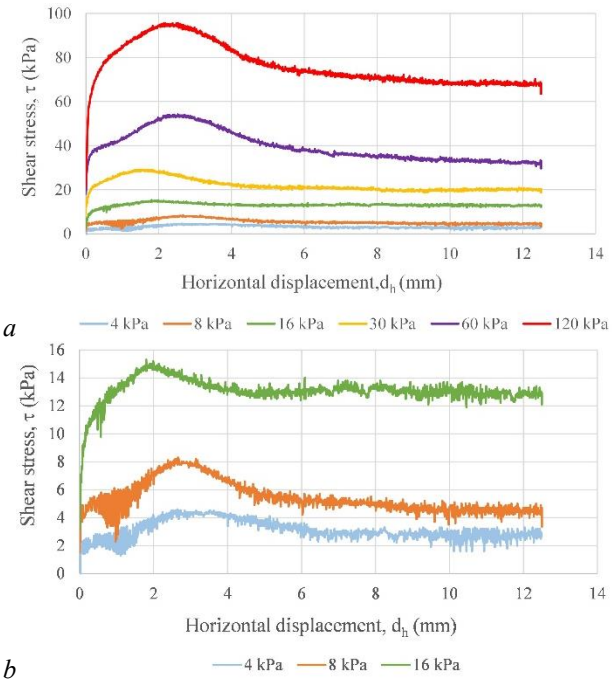

Figure 4. Shear stress- shear displacement results of the DS tests at a) all range of vertical effective stresses, b) low vertical effective stresses.

All direct tests show a clearly pronounced shear resistance peak and subsequent strain softening (Figure 4). The higher the effective vertical consolidation stress, the higher the peak and residual shear resistance. Figure 4b shows shear strength at low effective normal stresses from 4 to 16 kPa. The values of the test results for peak and residual conditions show a non-linear relationship, over the entire stress range of effective normal stresses (Figure 6b).

The test results obtained using triaxial tests are presented in Figure 5. Mean effective stress and deviatoric stress are calculated according to MIT principle (Lambe, 1967). For better comparison with the results obtained with DS and RSA, peak and residual values of shear strength obtained through triaxial tests (Figure 6c) were converted to the equivalent vertical and shear stress that would correspond to shear state obtained using the equipment with predefined shear surface.

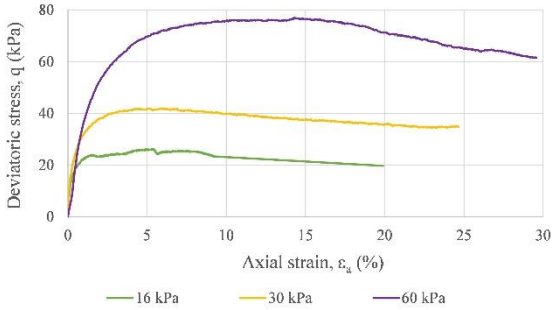

Figure 5. Deviatoric stress- axial strain results of the TX tests.

Figure 7 shows the peak and residual shear strength values for different vertical effective stresses according to the test results for all testing devices. The peak shear strength values obtained with the TX and RSA devices are close to each other, while the highest values were obtained with the DS device. The highest value of residual shear strength was obtained with the RSA device, while the values for the TX and DS devices were close to each other. Regardless of the testing device, the tests have the mean square error (R^2) greater than 0.87 (Figure 6).

The calculated effective friction angle for the peak and critical state obtained with different devices is analysed. The peak and residual friction angles obtained with the DS were 44° and 35° respectively for low effective normal stresses and reduced to 40° and 28° for higher stresses. The peak friction angle obtained with the DS is the highest, while the residual friction angle is the lowest among the used devices.

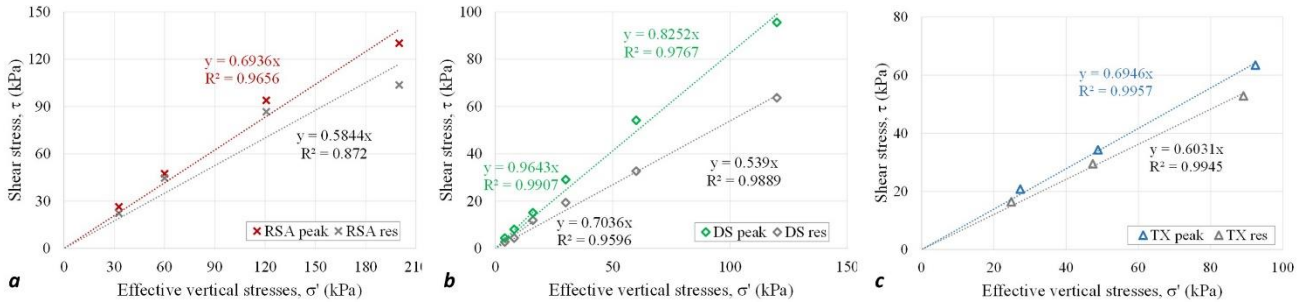

Figure 6. Mohr-Coulomb saturated shear strength envelope of sand obtained in the: a) ring shear tests, b) direct shear tests, c) triaxial tests.

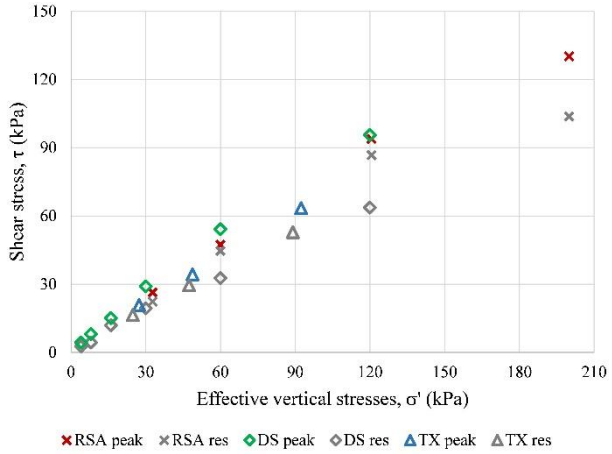

Figure 7. Peak and critical shear strength values of sand for different vertical effective stresses according to test results on all testing devices.

The peak value of the effective friction angle is between 40° and 35°, while the residual value is between 31° and 28° for higher stresses for the different devices.

It should be noted that the soil critical state is reached at different displacements depending on the type of the testing device (Figures 3, 4, and 5). For the DS and RSA tests, the critical state is reached in the range of 3 to 9 mm depending on the effective vertical stress value.

3 CONCLUSIONS

The paper dealt with the characterization of the sandy soil shear strength used in the small-scale physical models. Ring shear, direct shear, and triaxial tests were performed to investigate the differences in terms of friction angle under a range of stresses corresponding to the overburden stresses in the small-scale model and the real slope.

The paper showed that the experimental tests are fully reproducible as it concerns both the specimen preparation procedure and the testing technique.

The comparison between the results obtained with the different devices was made based on the residual and peak shear strength obtained and by calculating the effective friction angle. The test results indicate that the higher the effective vertical consolidation stress, the higher the peak and residual shear strength. The preliminary results of the tests indicate that the shear strength depends on the magnitude of the effective stresses and that as the stress level increase, the friction angle decreases. The ring shear device and triaxial devices show similar peak stress envelope while residual envelope is closer for direct shear and triaxial devices. A difference was found between the friction angle of sand at small normal stresses and at large normal stresses, indicating the need to use different values for the friction angle in the numerical modelling of the small-scale model and the real slope.

The results obtained in this study will be implemented in the future numerical modelling activities: while the shear strength characteristics obtained at relatively low confining pressures will be useful for a better understanding of small-scale slope models, the results obtained under higher stresses will be useful for numerical studies of real-size slopes.

ACKNOWLEDGEMENTS

The research presented in this paper was supported by Croatian Science Foundation under the Project IP-2018-01-1503. This work has been supported in part by the Ministry of Science, Education and Sports of the Republic of Croatia under the project Research Infrastructure for Campus-based laboratories at the University of Rijeka, number RC.2.2.060001. The project has been co-funded from the European Fund for Regional Development (ERDF). This paper was funded by the University of Rijeka under the project ZIP-UNIRI-1500-1-22 and partially supported by the project uniri-mladi-tehnic-22-62. This paper has been supported by the International Consortium on Landslides under the IPL-256 and IPL-265 projects. These supports are gratefully acknowledged.

REFERENCES

Castellanos, B. A., & Brandon, T. L. (2013). A Comparison Between the Shear Strength Measured with Direct Shear and Triaxial Devices on Undisturbed and Remolded Soils. *18th International Conference on Soil Mechanics and Geotechnical Engineering (Paris)*.

Chakraborty, T., & Salgado, R. (2010). Dilatancy and Shear Strength of Sand at Low Confining Pressures. *Journal of Geotechnical and Geoenvironmental Engineering*, *136*(3), 527–532. https://doi.org/10.1061/(ASCE)GT.1943-5606.0000237.

Cuomo, S., Foresta, V., & Moscariello, M. (2016). Shear strength of a pyroclastic soil measured in different testing devices. In *Volcanic Rocks and Soils* (1st Edition, p. 25).

Fukushima, S., & Tatsuoka, F. (1984). Strength and Deformation Characteristics of Saturated Sand at Extremely Low Pressures. *Soils and Foundations*, *24*(4), 30–48. https://doi.org/https://doi.org/10.3208/sandf1972.24.4_30.

Jagodnik, V., & Arbanas, Ž. (2022). Cyclic Behaviour of Uniform Sand in Drained and Undrained Conditions at Low Confining Stress in Small-Scale Landslide Model. *Sustainability*, *14*(19). https://doi.org/10.3390/su141912797.

Jagodnik, V., Kraus, I., Ivanda, S., & Arbanas, Ž. (2020). Behaviour of Uniform Drava River Sand in Drained Condition—A Critical State Approach. *Applied Sciences*, *10*(17). https://doi.org/10.3390/app10175733.

Ladd, R. S. (1978). Preparing Test Specimens Using Undercompaction. *Geotechnical Testing Journal*, *1*, 16–23.

Lambe, W. T. (1967). Stress Path Method. *Journal of the Soil Mechanics and Foundations Division*, *93*(6), 309–331. https://doi.org/10.1061/JSFEAQ.0001058.

Laurent, L., Isam, S., & Marwan, A. M. (2006). Failure and Dilatancy Properties of Sand at Relatively Low Stresses. *Journal of Engineering Mechanics*, *132*(12), 1396–1399. https://doi.org/10.1061/(ASCE)0733-9399(2006)132:12(1396).

Oštrić, M., Sassa, K., Ljutić, K., Vivoda, M., He, B., & Takara, K. (2014). Manual of transportable ring shear apparatus, ICL- 1. *Proceedings of 1st Regional Symposium on Landslides in the Adriatic-Balkan Region "Landslide and Flood Hazard Assessment,"* 1–4.

Pajalić, S., Peranić, J., Maksimović, S., Čeh, N., Jagodnik, V., & Arbanas, Ž. (2021). Monitoring and Data Analysis in Small-Scale Landslide Physical Model. *Applied Sciences*, *11*(11). https://doi.org/10.3390/app11115040.

Peranić, J., & Arbanas, Ž. (2020). Impact of the wetting process on the hydro-mechanical behavior of unsaturated residual soil from flysch rock mass: preliminary results. *Bulletin of Engineering Geology and the Environment*, *79*(2), 985–998. https://doi.org/10.1007/s10064-019-01604-0.

Peranić, J., Čeh, N., & Arbanas, Ž. (2022). The Use of Soil Moisture and Pore-Water Pressure Sensors for the Interpretation of Landslide Behavior in Small-Scale Physical Models. *Sensors*, *22*(19). https://doi.org/10.3390/s22197337.

Peranić, J., Moscariello, M., Cuomo, S., & Arbanas, Ž. (2020). Hydro-mechanical properties of unsaturated residual soil from a flysch rock mass. *Engineering Geology*, *269*, 105546. https://doi.org/https://doi.org/10.1016/j.enggeo.2020.105546.

Ponce, V. M.-, & Bell, J. M. (1971). Shear Strength of Sand at Extremely Low Pressures. *Journal of the Soil Mechanics and Foundations Division*, *97*(4), 625–638. https://doi.org/10.1061/JSFEAQ.0001578.

Shaoli, Y., Sandven, R., & Grande, L. (2003). Liquefaction of sand under low confining pressure. *Journal of Ocean University of Qingdao*, *2*(2), 207–210. https://doi.org/10.1007/s11802-003-0053-9.

Vivoda Prodan, M., & Arbanas, Ž. (2020). Analysis of the Possible Reactivation of the Krbavčići Landslide in Northern Istria, Croatia. In *Geosciences* (Vol. 10, Issue 8). https://doi.org/10.3390/geosciences10080294.

Vivoda Prodan, M., Mileusnić, M., Mihalić Arbanas, S., & Arbanas, Ž. (2016). Influence of weathering processes on the shear strength of siltstones from a flysch rock mass along the North Croatian Adriatic Coast. *Bulletin of Engineering Geology and the Environment*, *in press*.

Vivoda Prodan, M., Peranić, J., Pajalić, S., & Arbanas, Ž. (2023). Physical Modelling of Rainfall-Induced Sandy and Clay-Like Slope Failures. *Advances in Materials Science and Engineering*, *2023*, 3234542. https://doi.org/10.1155/2023/3234542.

Winters, K. E., Taylor, O.-D. S., Berry, W. W., Rowland, W. R., & Antwine, M. D. (2016). Cohesionless Soil Fabric and Shear Strength at Low Confining Pressures. In *Geo-Chicago 2016* (pp. 212–221). https://doi.org/10.1061/9780784480151.022.